Autooxidation of tetrachlorohydroquinone in aqueous media

L. M. Pisarenko

N. N. Semenov Institute of Chemical Physics, Russian Academy of Sciences,
4 ul. Kosygina, 117977 Moscow, Russian Federation.
Fax: +7 (095) 938 2156. E-mail: kasaikina@chph.ras.ru

The oxidation of tetrachlorohydroquinone in an aqueous solution at pH 7.40 is an autocatalytic reaction (sigmoid kinetic curves). The interaction of the tetrachloro-1,4-semiquinone radical anion with dioxygen occurs with the rate constant k_2 equal to 9±3 L mol^{-1} s^{-1} (22—37 °C). Superoxide dismutase does not affect the maximum rate of tetrachlorohydroquinone oxidation.

Key words: tetrachlorohydroquinone, tetrachloro-1,4-benzoquinone, tetrachloro-1,4-semiquinone radical anions, autooxidation, kinetics, superoxide dismutase.

Quinones are present in almost all respiratory cells of animals and plants. More than 1500 quinones possess antitumor activity,[1,2] which resulted in their wide use as antitumor medicines. However, such important parameters of quinones and hydroquinones as rate constants of the reaction of quinone with hydroquinone (k_1), of disproportionation of semiquinone radical anions (k_{-1}), and of interaction of semiquinone radical anions with dioxygen (k_2) are insufficiently studied. The number of works devoted to studying in detail the oxidation of hydroquinones in aqueous media is limited.[3] The rate constants of disproportionation of many semiquinone radical anions in aqueous media have recently been determined[4] by a pulse radiolysis technique.

This work is devoted to the oxidation of tetrachlorohydroquinone in an aqueous solution. Published data on the oxidation of this compound are scarce. Only the rate of absorption of dioxygen measured by the Clark electrode is presented.[5] Tetrachlorohydroquinone was obtained[5] directly in an oxidative cell in 0.1 *M* Tris-HCl buffer (pH 7.40) by the reduction of tetrachloro-1,4-benzoquinone (100 mmol L^{-1}) with sodium tetrahydridoborate (200 mmol L^{-1}) at 20 °C and then, without the subsequent isolation of hydroquinone from the reaction mixture, the rate of dioxygen absorption was measured as a value 30-fold higher than that obtained in this work.

Experimental

Tetrachloro-1,4-benzoquinone (Q) (Sigma) and superoxide dismutase (SOD) (Sigma) were used. Tetrachlorohydroquinone (QH_2) was obtained by the reduction of Q with zinc powder (commercially available) in AcOH with heating. QH_2 was oxidized in a 0.05 *M* phosphate buffer (pH 7.40) purified from traces of metals with variable valence using Chelex-100 reagent (Bio-Rad, Richmond (CA), USA). Absorption of O_2 during oxidation of QH_2 was studied on a Yellow Springs Instrument Co Model 5300 Biological Oxygen Monitor with a Clark electrode. The concentration of tetrachloro-1,4-semiquinone radical anions ($Q^{\cdot -}$) during oxidation of QH_2 in the phosphate buffer at 22 °C was monitored by ESR (Varian E-12) and UV spectroscopy. The ESR spectrum of the $Q^{\cdot -}$ radical anion is a singlet, ΔH = 0.80±0.05 G, g = 2.00535±0.00001. UV spectra during oxidation of QH_2 in the phosphate buffer were recorded on a Specord UV-VIS spectrophotometer in thermostatted cells. Reference solutions were prepared in different systems for different methods of analysis: for recording UV spectra, [QH_2] = 1 · 10^{-2} mol L^{-1} in the MeOH + 1 · 10^{-3} *N* HCl system, [Q] = 1 · 10^{-3} mol L^{-1} in MeOH; for recording ESR spectra, [QH_2] = 5 · 10^{-3} mol L^{-1} in Bu^{t}OH, [Q] = 1 · 10^{-2} mol L^{-1} in DMSO; and for oxidation on the Clark electrode, [QH_2] = 2.4 · 10^{-2} mol L^{-1} in the MeOH +

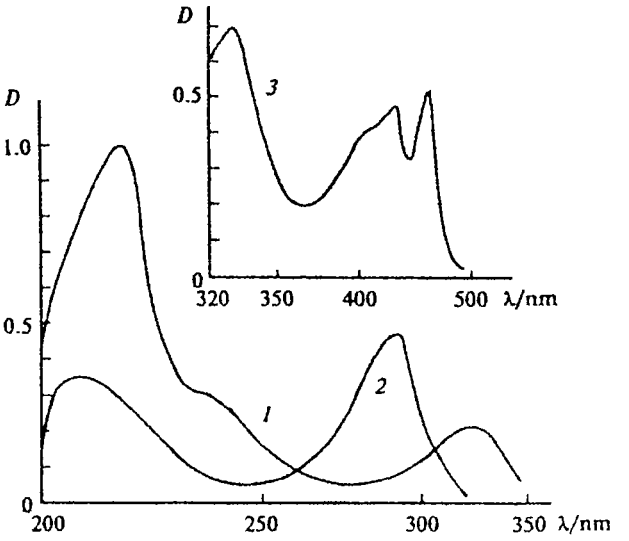

Fig. 1. UV spectra of QH_2 (*1*), Q (*2*), and $Q^{\cdot -}$ (*3*) in the phosphate buffer (22 °C): *1*, [QH_2] = 30 μmol L^{-1}, λ_{max} = 218 nm, ε = 30000 L mol^{-1} cm^{-1}; λ_{max} = 327 nm, ε = 5800 L mol^{-1} cm^{-1}; *2*, [Q] = 20 μmol L^{-1}, λ_{max} = 204 nm, ε = 17000 L mol^{-1} cm^{-1}; λ_{max} = 294 nm, ε = 21000 L mol^{-1} cm^{-1}; and *3*, [$Q^{\cdot -}$] = 78 μmol L^{-1}, λ_{max} = 461 nm, ε = 6600 L mol^{-1} cm^{-1}.

Translated from *Izvestiya Akademii Nauk. Seriya Khimicheskaya*, No. 5, pp. 890—895, May, 1999.

1066-5285/99/4805-0881 $22.00

$1 \cdot 10^{-3}$ *N* HCl system, [Q] = $0.6 \cdot 10^{-3}$ mol L^{-1} in DMSO. The extinction coefficient of Q was determined in the phosphate buffer + MeOH (3 : 1) mixture because of its poor solubility in the pure buffer. The extinction coefficient of $Q^{\cdot -}$ was determined from the ESR and UV spectra obtained during the oxidation of QH_2 (100 mmol L^{-1}) in the phosphate buffer at 22 °C. The UV spectra of QH_2, Q, and $Q^{\cdot -}$ are presented in Fig. 1.

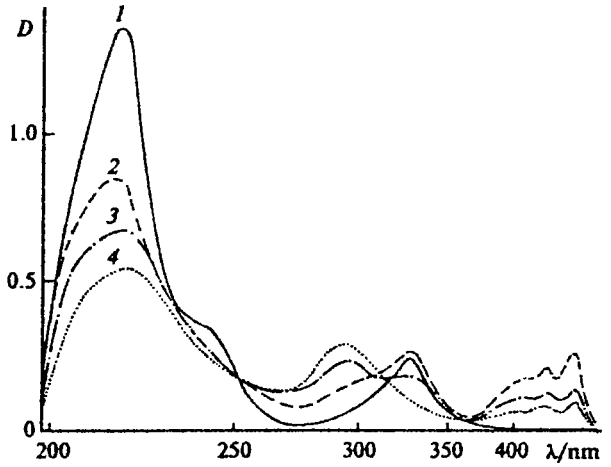

Fig. 2. UV spectra recorded during oxidation of QH_2 (45 μmol L^{-1}) in the phosphate buffer (22 °C), cell thickness 1 cm: *1*, at the beginning of oxidation; *2*, after 24 min; *3*, after 32 min; and *4*, after 46 min.

Results and Discussion

The UV spectra for different stages of oxidation of QH_2 (45 μmol L^{-1}) in the phosphate buffer at 22 °C are presented in Fig. 2. One of the absorption bands of QH_2 (λ_{max} = 327 nm) does not bear information, because the $Q^{\cdot -}$ radical anion appearing during the QH_2 oxidation also absorbs in this region. The absorption band of QH_2 in the region of 218 nm bears little information and, hence, it was used only as a control of the concentration of QH_2 introduced. The products of QH_2 oxidation, whose structure was not studied, contribute to this spectral region. Change in the concentrations of Q and $Q^{\cdot -}$ were monitored by absorption bands of Q (λ_{max} = 294 nm) and $Q^{\cdot -}$ (λ_{max} = 461 nm). The ESR and UV spectroscopic data for the $Q^{\cdot -}$ radical anion at 461 nm are presented in Fig. 3. The extinction coefficient of the $Q^{\cdot -}$ radical anions was determined from the slope angle: at λ = 461 nm, ε = 6600 L mol^{-1} cm^{-1}. The good coincidence of the shapes of the kinetic curves for accumulation and consumption of $Q^{\cdot -}$ radical anions obtained by different methods (ESR and UV spectra) under the same conditions of QH_2 oxidation indicates that the oxidation products have no effect on the shape and position of the absorption band at 461 nm; therefore, the determination of the concentration of $Q^{\cdot -}$ radical anions is always very accurate. The curves of the changing concentrations of QH_2, $Q^{\cdot -}$, Q, and O_2 during QH_2 oxidation are presented in Fig. 4 (by the data of UV spectroscopy and measurements using the Clark electrode).

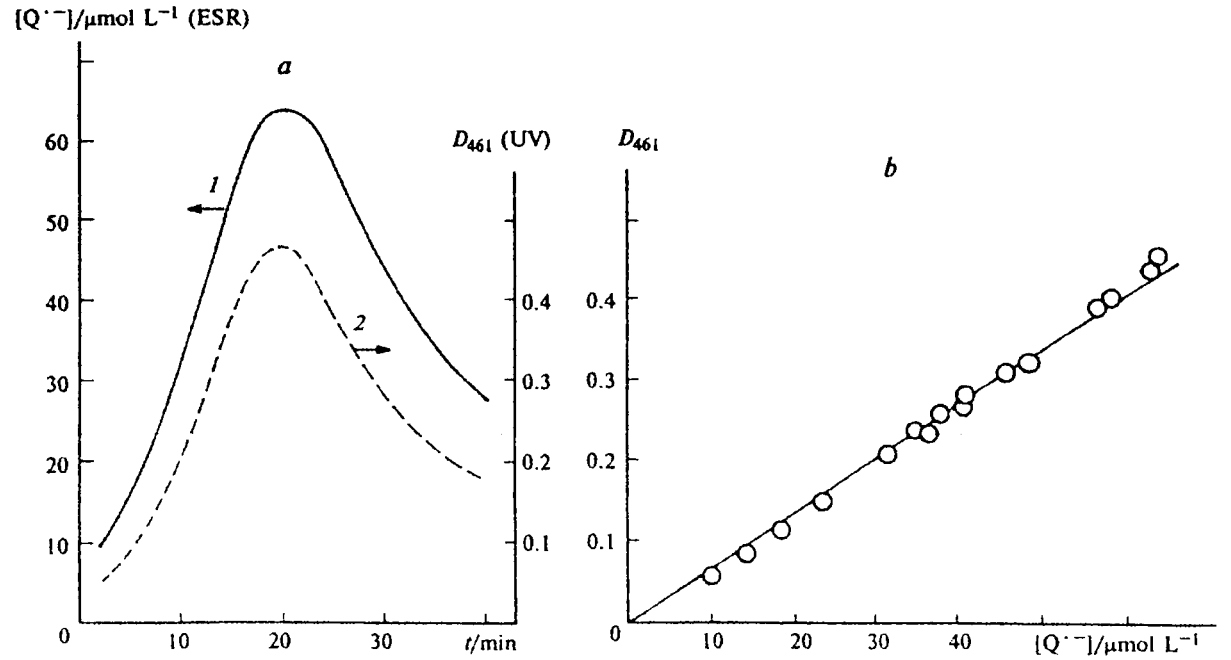

Fig. 3. *a*. Changes in the concentration of $Q^{\cdot -}$ radical anions during oxidation of QH_2 (100 mmol L^{-1}) in the phosphate buffer at 22 °C by ESR (*1*) and UV spectroscopy (*2*) data. *b*. Concentration dependence of the optical density of $Q^{\cdot -}$ radical anions (λ_{max} = 461 nm).

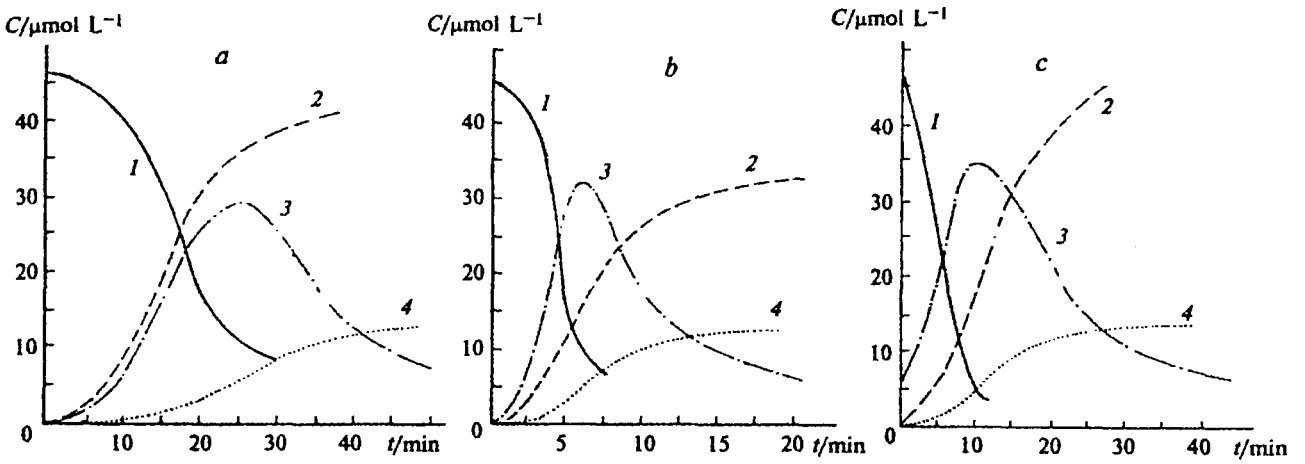

Fig. 4. Kinetic curves of consumption of QH_2 (*1*), absorption of O_2 (*2*), accumulation and consumption of $Q^{\cdot -}$ (*3*), and accumulation of Q (*4*) during oxidation of QH_2 (45 μmol L^{-1}) in the phosphate buffer at different temperatures (*a*, *b*) and after addition of Q (*c*): *a*, 22 °C; *b*, 37 °C; and *c*, 22 °C, [Q] = 1 μmol L^{-1}.

According to the material balance, the following correlation between the initial concentration of QH_2 ($[QH_2]_0$) and the concentrations of products of its oxidation should be fulfilled in the oxidizing system at any moment:

$$[QH_2]_0 \geq [QH_2]_t + [Q^{\cdot -}] + [Q] + [P], \quad (1)$$

where $[QH_2]_t$ is the current concentration of QH_2, and P are unknown products of QH_2 oxidation. It follows from inequality (1) that the $[QH_2]_t$ value satisfies the correlation

$$[QH_2]_t \leq [QH_2]_0 - [Q^{\cdot -}] - [Q] - [P]. \quad (2)$$

Since the concentration of the $Q^{\cdot -}$ radical anions can be determined with a high accuracy (their contribution to the reaction course is the major one, according to Fig. 4), and the concentration of Q is low (especially in the first half of the oxidation process), it is probable that the concentration of products P at this stage of oxidation is also low. Therefore, we can conclude that the kinetic curve of QH_2 consumption found by Eq. (2) reflects sufficiently accurately the real oxidation process.

As can be seen in Fig. 4, the kinetic curves are sigmoid, which is characteristic of autocatalytic processes. The kinetic curves obtained in other experiments on QH_2 oxidation have similar sigmoid shapes (Table 1).

The dependences of the maximum rate of hydroquinone oxidation (R_{O_2}) on $[QH_2]$ at different temperatures are presented in Fig. 5. The linear character of the dependences indicates that R_{O_2} is a function of the concentration of QH_2:

$$R_{O_2} = f[QH_2]. \quad (3)$$

The effective rate constants of oxidation $k_{eff} = 2 \cdot 10^{-3}$ s^{-1} (37 °C) and $1 \cdot 10^{-3}$ s^{-1} (22 °C) were obtained from the slopes of the corresponding lines. The linear dependence of R_{O_2} on $[QH_2]$ suggests that O_2 is absorbed by the $Q^{\cdot -}$ radicals (Scheme 1, reaction *2*) which are formed in reaction *1*.

In this case, according to Eq. (3), the rate of QH_2 oxidation is determined by the value

$$k_2[Q^{\cdot -}][O_2] = k_{eff}[QH_2]. \quad (4)$$

Table 1. Maximum rates of consumption of QH_2, absorption of O_2, accumulation and consumption of $Q^{\cdot -}$, and accumulation of Q during oxidation of QH_2 (45 μmol L^{-1}) in the phosphate buffer at different temperatures and different concentrations of Q additives

T /°C	$[Q]_0$ /μmol L^{-1}	$R_{QH_2} \cdot 10^8$	$R_{O_2} \cdot 10^8$	$R_{Q^{\cdot -}}^{accum} \cdot 10^8$	$R_{Q^{\cdot -}}^{cons} \cdot 10^8$	$R_Q \cdot 10^8$	τ* /min
		mol L^{-1}					
22	0	2.7	4.2	3.9	2.3	0.9	24
22	0.5	4.9	—	5.0	2.5	1.4	15
22	1.0	8.3	4.9	6.3	2.7	1.9	10
22	2.5	9.6	6.3	7.2	3.5	2.1	10
22	4.0	19.0	7.2	7.9	4.0	2.0	7
37	0	24.0	7.1	15.0	6.0	2.6	6

* Inflection point.

Scheme 1

$QH_2 \rightleftharpoons {}^{-}OH + H^+ \rightleftharpoons Q^{2-} + 2\,H^+$ (reaction *0*)

$QH_2 + Q \longrightarrow Q^{\cdot -} + Q^{\cdot -} + 2\,H^+$ (reaction *1*)

$2\,H^+ + Q^{\cdot -} + Q^{\cdot -} \longrightarrow QH_2 + Q$ (reaction *−1*)

$Q^{\cdot -} + O_2 \longrightarrow Q + O_2^{\cdot -}$ (reaction *2*)

It therefore follows that

$$k_2 = k_{eff}[QH_2]/([Q^{\cdot -}][O_2]). \quad (5)$$

The information on the concentrations of QH_2, $Q^{\cdot -}$, and O_2 (see Fig. 4, *a*, *b*) made it possible to find very important values from Eq. (5): rate constants of the interaction of the $Q^{\cdot -}$ radical anions with dioxygen (k_2) at 22 and 37 °C, which are equal to 8.9 L mol^{-1} s^{-1} (22 °C) and 6.0 L mol^{-1} s^{-1} (37 °C). Therefore, the k_2 value for the $Q^{\cdot -}$ radical anion is the same at different temperatures within the error limits. It is seen in Fig. 4, *a*—*c* that the kinetic curves of the changing concentration of $Q^{\cdot -}$ radical anions during QH_2 oxidation pass through a maximum in all cases. The position of the maximum (inflection point) corresponds to the moment at which the rate of accumulation of the $Q^{\cdot -}$ radical anions is equal to the rate of their consumption, *i.e.*, $d[Q^{\cdot -}]/dt = 0$. The concentration of QH_2 in the system is low to the moment corresponding to the point of the maximum. If the consumption of the $Q^{\cdot -}$ radical anions is considered to be mainly due, in this case, to reaction *2* (see Scheme 1), we can write

$$R_{Q^{\cdot -}}^{cons} = k_2[Q^{\cdot -}][O_2]; \quad (6)$$

it therefore follows that

$$k_2 = R_{Q^{\cdot -}}^{cons}/([Q^{\cdot -}][O_2]). \quad (7)$$

According to the data in Table 1 and Fig. 4, *a*—*c*, k_2 = 6 L mol^{-1} s^{-1} (22 °C) and 11.7 L mol^{-1} s^{-1} (37 °C). Thus, the k_2 values found by different methods are close, and the average k_2 value within the experimental error is equal to 9±3 L mol^{-1} s^{-1}.

The rate constant k_2 for the radical anion under study differs strongly (by 4 orders of magnitude) from the k_2 value for the radical anion of unsubstituted hydroquinone.[3] This is probably related to the specificity of the structure of the $Q^{\cdot -}$ radical anion, with all H atoms substituted by electron-withdrawing Cl atoms, due to which its external shell is a continuous electronegative zone; the latter results, most likely, in such a low k_2 value. As a result, the interaction of tetrachlorosemiquinone radical anions with dioxygen occurs with low rates and is characterized by very low activation energies.

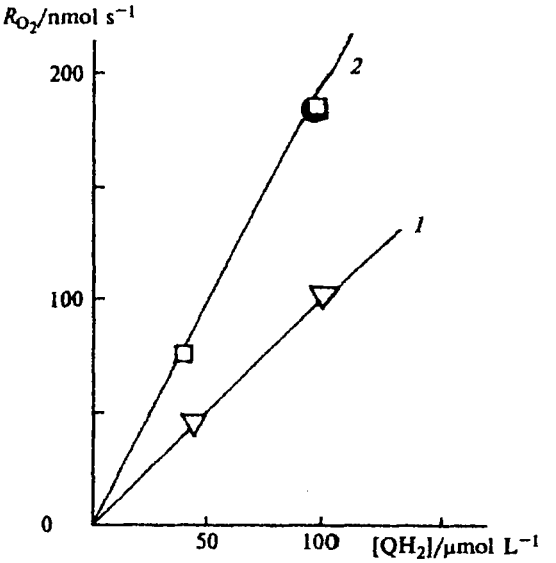

Fig. 5. Concentration dependences of the maximum oxidation rate of hydroquinone (R_{O_2}) at 22 °C (*1*) and 37 °C (*2*); ● is oxidation of QH_2 in the presence of 500 SOD units.

In reaction *2* (see Scheme 1), $O_2^{\cdot -}$ radical anions are formed, which can substantially affect the oxidation of QH_2. As follows from the published data, the oxidation of hydroquinone is completely retarded by the inverse reaction:

$Q + O_2^{\cdot -} \longrightarrow Q^{\cdot -} + O_2$. (reaction *−2*)

Reaction *−2* proceeds with a high rate, suppressing the direct reaction *2*, because $k_{-2} >> k_2$.[3] The superoxide dismutase enzyme reacts with the $O_2^{\cdot -}$ radical anions at a high rate ($k_3 = 5 \cdot 10^9$ L mol^{-1} s^{-1}) to form hydrogen peroxide and inactive products[6] (conventionally designated as (SOD)) and thus efficiently removing the $O_2^{\cdot -}$ radical anions from the system

$SOD + O_2^{\cdot -} \longrightarrow H_2O_2 + (SOD)$. (reaction *3*)

Therefore, the introduction of SOD into the reaction system makes it possible to estimate the contribution of reaction *−2* to the oxidation of QH_2. When QH_2 (100 μmol L^{-1}) is oxidized in the phosphate buffer at 37 °C in the presence of 500 SOD units, the maximum rate of QH_2 oxidation remains unchanged ($R_{O_2} = R_{O_2,SOD} = 1.8 \cdot 10^{-7}$ L mol^{-1} s^{-1}, see Fig. 5). This confirms that reaction *−2* is insignificant in QH_2 oxidation.

The inflection point on the kinetic curve of changing $[Q^{\cdot -}]$ corresponds to the maximum rate of Q accumulation regardless of the temperature and Q additives to oxidized QH_2. At this point, the ratio of the concentration of the $Q^{\cdot -}$ radical anions to that of Q is always constant: $[Q^{\cdot -}]/[Q] = 6 \pm 1$. This implies that the inflection point corresponds to the moment when only 1/6

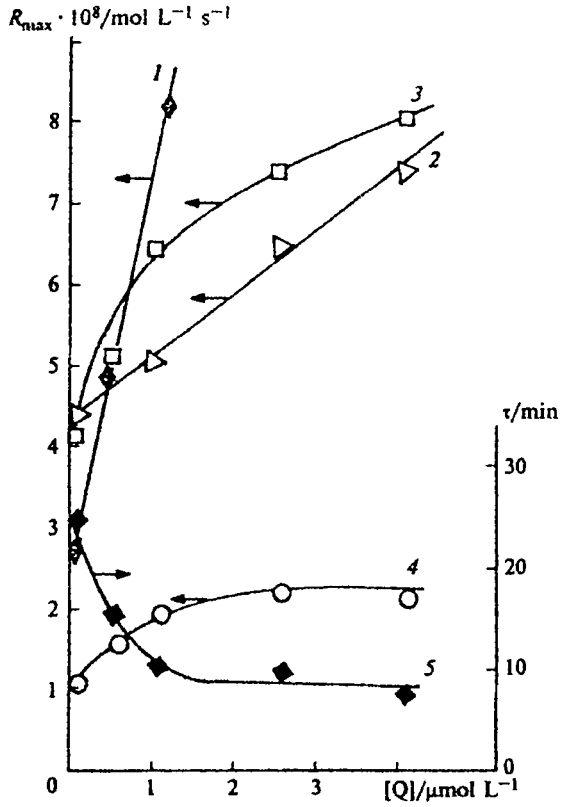

Fig. 6. Changes in the maximum rates of consumption of QH_2 (*1*), absorption of O_2 (*2*), accumulation of $Q^{\cdot -}$ (*3*) and Q (*4*), and position of the inflection point (τ) of the oxidation of QH_2 (*5*) at different concentrations of Q additives during oxidation of QH_2 (45 μmol L^{-1}) in the phosphate buffer at 22 °C (data in Table 1).

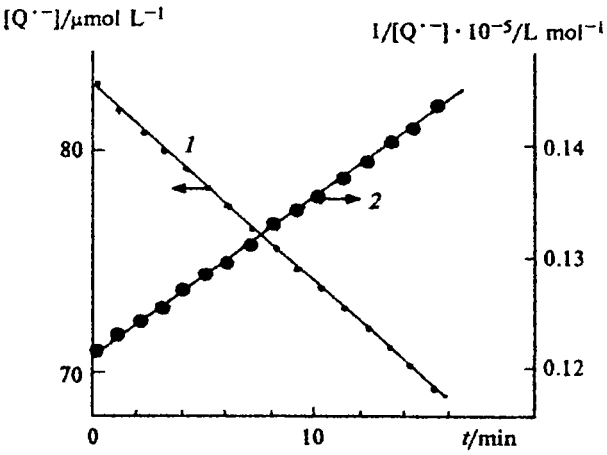

Fig. 7. Kinetic curve (*1*) of decay of $Q^{\cdot -}$ radicals (82 μmol L^{-1}) formed in the reaction of QH_2 (50 μmol L^{-1}) with Q (62 μmol L^{-1}) in an inert medium (Ar) in the phosphate buffer at 22 °C and its anamorphosis (*2*) in the coordinates $1/[Q^{\cdot -}]$—*t*.

of the Q formed in reaction *2* (see Scheme 1) remains in the oxidized system (Q accumulates). The remaining portion of Q again enters reaction *1*. This multiple participation of Q in the reaction with QH_2 is the reason for its low concentration. This occurs until QH_2 is present in the system.

The addition of Q to QH_2 results in the acceleration of the QH_2 oxidation (see Fig. 4, *c*). Based on the data in Table 1, we plotted the dependences of the changing rates of QH_2 consumption, $Q^{\cdot -}$ and Q accumulation, and O_2 absorption and the position of the inflection point for QH_2 oxidation on the concentration of Q additives (Fig. 6). The rates of QH_2 consumption, $Q^{\cdot -}$ and Q accumulation, and O_2 absorption in the presence of Q additives increase in different manners. Within the Q concentration range below 1 μmol L^{-1}, all rates increase, and the time of achievement of the inflection point shortens sharply. At a content of Q > 1 μmol L^{-1}, only the rate of Q accumulation remains unchanged, and this does not change the time of achievement of the inflection point.

It was shown by ESR spectroscopy that in an inert medium (Ar) the $Q^{\cdot -}$ radical anions that appeared in the reaction of QH_2 with Q decay in reaction -1^* at an average rate of 1% min^{-1} to form products, whose structure was not studied:

$$2\,H^+ + Q^{\cdot -} + Q^{\cdot -} \longrightarrow \text{Products.} \qquad \text{(reaction } -1^*\text{)}$$

As follows from Fig. 7, the $Q^{\cdot -}$ radical anions decay in a second-order reaction with the rate constant k_{-1^*} = 2.1 L mol^{-1} s^{-1} according to the equation

$$1/[Q^{\cdot -}] = 1/[Q^{\cdot -}]_0 + 2.1t. \qquad (8)$$

The k_{-1^*} rate constant is very low and, perhaps, the $Q^{\cdot -}$ radical anions decay *via* this channel only when other, faster routes are absent.

It is well known that benzoquinones and hydroquinones at a molar ratio of 1 : 1 form quinhydrones. Benzoquinone and hydroquinones in quinhydrones retain their individual character (mobility). In this case, the presence of electron-withdrawing Cl atoms in benzoquinone and hydroquinone results in the formation of very stable quinhydrones. The UV spectra of solutions of Q (33 μmol L^{-1}) and QH_2 (31 μmol L^{-1}) before and after mixing in an O_2 atmosphere at 22 °C are presented in Fig. 8. The optical density of the spectrum obtained after mixing Q with QH_2 in the region of 218 nm is the sum of the optical densities of Q and QH_2. A new band close to the absorption band of benzoquinone (294 nm) appears in the region of 300 nm. The bands in the region of 400 nm and further belong to the $Q^{\cdot -}$ radical anions only. The formation of quinhydrone results in an unusual change in the optical densities during the QH_2 oxidation. Immediately after mixing of Q and QH_2, the optical density in the region of 218 nm begins to decrease, and the absorption band in the region of 294 nm disappears. A new absorption band appears at 300 nm, and its optical density increases rapidly (~2 min) by a

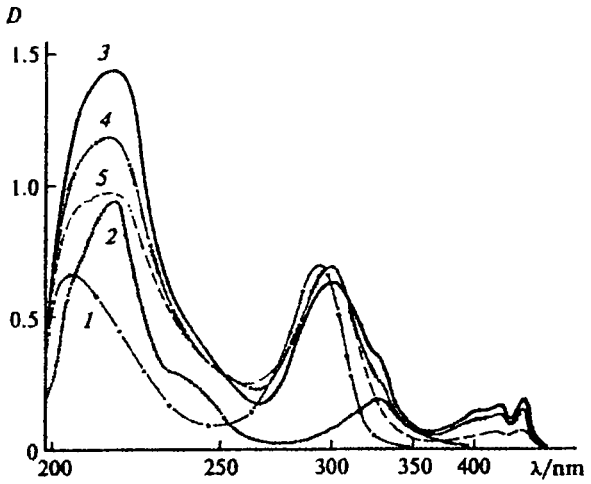

Fig. 8. UV spectrum of Q (33 μmol L^{-1}) (*1*) and QH_2 (31 μmol L^{-1}) (*2*) in the system phosphate buffer + MeOH (3 : 1) in an O_2 atmosphere at 22 °C and Q + QH_2 immediately after mixing (*3*), after ~7 min (*4*), and after ~20 min (*5*).

Table 2. Concentration of $Q^{\cdot -}$ radical anions formed during mixing of solutions of Q and QH_2 with different initial concentrations (22 °C)

Entry	[QH_2]	[Q]	[$Q^{\cdot -}$]	Medium
	μmol L^{-1}		/μmol L^{-1} (%)	(method)
1	31	33	29 (45)	O_2 (UV)
2	18	21	15 (38)	O_2 (UV)
3	62	50	82 (73)	Ar (ESR)
4	44	12	29 (52)	O_2 (UV)
5	42	15	36 (63)	Ar (ESR)
6	11	33	18 (41)	O_2 (UV)

very small value and then remains unchanged during the whole observed process of QH_2 oxidation (25 min). The behavior of the $Q^{\cdot -}$ radical anions is unusual. Their concentration within 6 min remained unchanged (the optical density at λ_{max} = 461 nm remains unchanged), and only afterwards does the $Q^{\cdot -}$ radical anions begin to be consumed. A similar spectral pattern is observed when solutions of Q and QH_2 with concentrations of 18 and 21 μmol L^{-1}, respectively, are mixed. When mixing solutions of Q and QH_2 with different initial concentrations, the shapes of the spectra and the kinetics of the behavior of the components are different. Thus, reaction *1** proceeds during the oxidation of QH_2 when the molar concentrations of the formed Q and remaining QH_2 are equalized:

$$Q + QH_2 \longrightarrow [Q...QH_2] \longrightarrow Q^{\cdot -}. \qquad \text{(reaction } 1^*\text{)}$$

The concentrations of the $Q^{\cdot -}$ radical anions formed during mixing of solutions of Q and QH_2 with different initial concentrations are presented in Table 2. When [Q] = [QH_2] (entries *1* and *2*) or [Q] is three-fold higher than [QH_2] (entry *6*), ~40% $Q^{\cdot -}$ radical anions appear in the system. If [QH_2] > [Q] by 1—3 times (entries *3*—*5*), 50—70% $Q^{\cdot -}$ radical anions are formed.

* * *

Thus, the oxidation of tetrachlorohydroquinone in the buffer solution with pH 7.40 occurs autocatalytically (sigmoid kinetic curves). The tetrachlorohydroquinone—tetrachloro-1,4-benzoquinone system is responsible for autocatalysis. The reaction of the tetrachloro-1,4-semiquinone radical anion with dioxygen occurs with k_2 = 9±3 L mol^{-1} s^{-1} (22—37 °C).

The author thanks V. A. Roginsky for critical remarks and interest in this work.

ESR studies were financially supported by Volkswagen Stifung (Grant 1/71149, 1996—1997).

References

1. J. S. Driscoii, G. F. Hazard, H. B. Wood, and A. Goidin, *Cancer Chemother.*, 1974, Rep. 4 (part 2), 1.
2. A. Brunmark and E. Cancdas, *J. Free Rad. Biol. Med.*, 1989, **7**, 435.
3. P. Ever, *Chem. Biol. Interactions*, 1991, **80**, 159.
4. V. A. Roginsky, L. M. Pisarenko, C. Michel, M. Saran, and W. Bors, *J. Chem. Soc., Faraday Trans.*, 1998, **94**, 1835.
5. P. J. O'Brien, *Chem. Biol. Interactions*, 1991, **80**, 1.
6. E. Cadenas, D. Mira, A. Brunmark, C. Lind, J. Segura-Aguilar, and L. Ernster, *J. Free Radicals Biol. Med.*, 1988, **5**, 71.

Received June 19, 1998;
in revised form October 20, 1998